GASEOUS OPTICAL CONTAMINATION OF THE SPACECRAFT ENVIRONMENT: A REVIEW

N. H. Tran, M. A. Maris and I. L. Kofsky
PhotoMetrics, Inc., 4 Arrow Dr., Woburn, MA, 01801

and E. Murad
Air Force Geophysics Laboratory, Hanscom AFB, MA, 01731

ABSTRACT

Interactions between the ambient atmosphere and orbiting spacecraft, sounding rockets, and suborbital vehicles, and with their effluents, give rise to optical (extreme UV to LWIR) foreground radiation which constitutes noise that raises the detection threshold for terrestrial and celestial radiations, as well as military targets. We review the current information on the on-orbit optical contamination. Its source species are created in interaction processes that can be grouped into three categories: 1) Reactions in the gas phase between the ambient atmosphere and desorbates and exhaust; 2) Reactions catalyzed by exposed ram surfaces, which occur spontaneously even in the absence of active material releases from the vehicles; and 3) Erosive excitative reactions with exposed bulk (organic) materials, which have recently been identified in the laboratory though not as yet observed on spacecraft. We also assess the effect of optical pumping by earthshine and sunlight of both reaction products and effluents.

INTRODUCTION

The optical "foreground" contamination from gases excited by the interaction with the atmosphere of orbiting vehicles and re-entry bodies (and some sounding rockets), and from molecules inadvertently outgassed and purposefully exhausted from these spacecraft, falls into the three broad categories listed in Table 1. Figure 1 schematizes these UV-visible-IR radiations, and identifies the currently-perceived principal emitting species.

EXCITATIVE REACTIONS OF MOLECULES IN THRUSTER ENGINE EXHAUST

The velocities of the combustion products of typical control rocket engines are as high as 11-12 km/s relative to the (1000K, 1 km/s mean thermal speed) oxygen atoms and nitrogen molecules that compose most of the atmosphere at low-earth orbital altitudes. Table 2 lists the center-of-mass kinetic energies in collisions of 3½ km/s expected exhaust species from present thruster types with stationary O and the order-of-magnitude less abundant (and also less reactive) N_2. (The energies of outgas species lie between those shown.) This energy is in principle available for overcoming potential barriers of exothermic chemical reactions and populating upper electronic, vibrational, and rotational states of the products, as well as for similarly exciting the exhaust molecules themselves.

Figure 2 is a flow chart of the procedure that we applied (1) in identifying from the many possible reactions those of the highest-mole fraction exhaust molecules that result in electronically excited products with radiative lifetimes less than about 1/10 second. (When the lifetime of the upper state is longer, the excited molecules spread over such long distances that surface radiances become below detection thresholds.) Reactions that fail to conserve spin angular momentum are less favored; T → E collisions generally have lower probability than excitative atom-interchange collisions; and the cross-sections for exothermic reactions (such as $NO + O \rightarrow NO_2^*$) generally decrease with increasing kinetic energy of the participants. The principal excitative reactions of thruster exhaust meeting the tests of Figure 2 appear in Table 3, and estimates of their cross-sections from an evaluation of literature sources appear in Reference 1.

In practice only a sparse laboratory database exists on excitative processes at the kinetic energies in Table 2, and ab initio theory is in general not reliable. An example of the uncertainties for even so simple a collision process as H_2O (X,000) + O → H_2O (ν1,ν2,ν3) + O can be seen in Figure 3. Reference 2 gives some recently measured cross-sections for vibrational excitation in collisions with 8 km/s O atoms of CO, CO_2, and CH_4, and for dissociations of these species with vibrational excitation of a product molecule.

EROSIVE / EXTRACTIVE REACTIONS

While the rates of erosion of several types of exposed spacecraft materials by oxygen atoms with orbital relative velocities have been measured (3), the extraction mechanisms are not well understood. Yields of infrared radiation from the vibrationally-excited CO, CO_2, and OH molecules produced from organic (and thin layer of contaminant-covered metal) surfaces by O bombardment have recently been reported to be in the 10^{-2}-10^{-1} range (4), and further laboratory measurements are expected shortly.

SURFACE-CATALYZED RECOMBINATION OF IMPINGING ATMOSPHERIC SPECIES

Visible and near-ultraviolet glows with radiances comparable with that of the natural nightglow have been found in the last few years to extend from the ram-directed surfaces of satellites in low earth orbits (see in particular Reference 5). These emissions appear to be a general property of spacecraft moving through the thermosphere and, by inference, of exo-reentry and launch vehicles also. Table 4 is a listing of the perceivedly highest-radiance glows induced at spacecraft surfaces. These emissions arise from chemiluminous recombination reactions of ambient atoms and molecules incident on windward exposed surfaces, where the gas densities are high (and may be increased by backscattering from the atmosphere at the lower orbital altitudes).

These radiations, with the exception of the vibrational cascades from NO and NO_2 (final four entries in Table 4, predicted but not yet observed), are tabulated in order of increasing emission wavelength (second column). The spatial extents of these glows (third column) were derived with the assumption that the excited species are thermally accommodated with the surface before effusing from it. The radiances in the molecular bands (fourth column) are in general no more than rough estimates, as the absolute excitation probabilities are in very few cases known (if any).

Two extremes of projections for passive measurement of the radiances of off-spacecraft glows, parallel and perpendicular to the recombination surface are illustrated in Figure 4. If the distance L over which the molecule emits most of its radiation is less than the characteristic linear dimension W of the surface, signal/noise will be higher in the first view projection. When the desorbed particles do not collide with the atmospheric gas this distance L is to a good approximation (mean normal velocity of the desorbate) x (radiative lifetime of its excited state(s)). Thus (as examples) electric dipole-permitted electronic transitions with typical lifetimes ~10^{-7} sec would take place over much less than a millimeter from the excitation surface, and thus would reflect the recombination characteristics of the components of the optical sensor; transitions from NO_2 ($^2B_1$, $^2B_2$) with their ~100 msec lifetimes would produce radiation over a few cm, as observed; and (an extreme case) O_2 in its 3700-sec lifetime a $^1\Delta_g$ state would radiate over pathlengths of more than a thousand km when these molecules desorb into the zenith hemisphere, and thus exhibit extremely low surface brightness. When L < W a "van Rhijn" gain can be achieved on optically-thin glows by use of projections of narrow fields of view near-parallel to extended recombination surfaces. When L > W, even if the internally-excited species is desorbed non-isotropically the radiance of its glow in most projections varies with L^{-2} (neglecting collisional depopulation, or upward pumping of the desorbate stream), that is, with the inverse square of its radiative lifetime. For example if the 12-sec lifetime O_2 (b) and 3700-sec O_2 (a) states generally accepted as resulting from recombination of O atoms are populated at equal rates, column brightnesses in the [assumed unquenched] a → X Infrared Atmospheric bands would be a factor 10^5 lower than those in the b → X Atmospheric bands.

Both astronomical and terrestrial-atmospheric optical backgrounds are always present, and appear also as scattering off structures lying in sensor fields of view (over and above the infrared thermal radiation from such structures). Noise due to the natural variability of these backgrounds is a limiting factor in detection of all off-surface glows; the longer-lived recombination radiations listed in

Tables 5 and 6 would provide inadequate signal above this noise no matter what projection, or instrument throughput, is brought to bear. This effect is included in Figure 4's flow chart for excitation and detectability of recombination glows. A reaction with desorption in an excited stated must be favored by the substrate; indeed, visible spacecraft glow has been found to be less intense off exposed polyethylene $(CH_2)_n$ and anodized aluminum than off paints that have unsaturated chemical bonds (compare the low rate of recombinations and deactivations on teflon $(CF_2)_n$ in the laboratory).

With the assumption that its collision with the exposed surface does not electronically excite the impinging orbital-atmospheric atom or molecule, the upper electronic states of product molecules of surface-catalyzed recombination can be identified from their standard potential diagrams. (Too few initially-excited species are present in the flow to the surface to result in significant recombination radiation.) The thus-accessible ultraviolet- and infrared-radiating states from reactions of $O(^3P)$, $N(^4S)$, and $NO(X^2P)$ are shown in Tables 5 and 6, which include information from a survey of the literature on excitative recombination at laboratory surfaces (5). The most recently identified radiative state--also populated by gas-phase recombination--is N_2 $(a^1\Pi_g)$ (6).

As noted above, only a small fraction of these optical features would be detectable by passive spectroradiometry against the celestial and terrestrial backgrounds. Several of the other upper states lend themselves to detection by laser-probing methods, as we have suggested previously (5,7).

The database on observations of these spacecraft surface-catalyzed recombination glows is reviewed in a separate presentation at this meeting (Paper E1-3; refer also to the report of a recent conference devoted to this topic (8)). The by far dominant feature at the readily experimentally-accessible visible wavelengths is the NO_2 $(^2B_1,^2B_2 \rightarrow X^2A_1)$ pseudocontinuum from reaction of O atoms with NO molecules (naturally present in the atmosphere, or as has been postulated formed at the surface by recombination of atmospheric N and O). While the emission--the "Lewis-Rayleigh afterglow"--is a well-known feature of both laboratory gas discharges and the natural lower-thermospheric airglow (which forms under "radiation-stabilized" conditions, and therefore peaks well to the blue of the surface recombination glow) (see Reference 5; in particular Table 3), the off-surface emission has only been recently--in response to the stimulus of optical data from spacecraft--been unambiguously identified in the laboratory (9,10).

REFERENCES

1. Kofsky, I. L., Barrett, J. L., Brownrigg, T. E., McNicholl, P. N., Tran, N. H., and Trowbridge, C. A., "Excitation and Diagnostics of Optical Contamination in the Spacecraft Environment," AFGL-TR-88-0293, Air Force Geophysics Laboratory, Hanscom AFB, Massachusetts, July, 1988.

2. Green, B. D., and Caledonia, G. E., "Laboratory Investigations of High Velocity Atom Interactions," PAPER III-2, Johns Hopkins Univ./ Applied Physics Laboratory Vehicle-Environment Interaction Workshop, Laurel, Maryland, February 21-22, 1989.

3. Leger, L. J., and Visentine, J. T., "A Consideration of Atomic Oxygen Interactions with the Space Station," J. SPACECRAFT ROCKETS, New York, Vol. 23, 1988, pg. 505.

4. Fraser, M. E., Holtzclaw, K. W., and Gelb, A., "Mechanisms of High Velocity Oxygen Atom Reactions with Material Surfaces," PAPER SM21A-03, AGU Conference abstract publ. in EOS, Vol. 69, No. 44, November, 1988, pg. 1377.

5. Kofsky, I. L., and Barrett, J. L., "Spacecraft Glows from Surface-Catalyzed Reactions," PLANET. SPACE SCI., Vol. 34, No. 8, 1986, pp. 665-681.

6. Kofsky, I. L., "Excitation of N_2 Lyman-Birge-Hopfield Bands Emission by Low Earth Orbiting Spacecraft," GEOPHYS. RES. LETT., Vol. 15, No. 3, March, 1988, pp. 241-244.

7. Kofsky, I. L., and Barrett, J. L., "Spacecraft Surface Glows," NUCL. INSTR. METHODS IN PHYS RES., Vol. B14, 1986, pg. 480.

8. Meng, C. I., Ed., "Vehicle-Environment Interaction Workshop," Proc. of Johns Hopkins Univ./ Applied Physics Laboratory Vehicle-Environment Interaction Workshop, Laurel, Maryland, February 21-22, 1989.

9. J. A. Halstead, Triggs, N., Chu, A.-L., and Reeves, R. R., "Creation of Electronically Excited States by Heterogeneous Catalysis," in GAS-PHASE CHEMILUMINESCENCE AND CHEMIIONIZATIONS, Ed. A. Fontijn, Elsevier, Amsterdam, 1985, pp. 307-326.

10. Chu, A.-L., Reeves, R. R., and Halstead, J. A., "Surface-Catalyzed Formation of Electronically Excited Nitrogen Dioxide and Oxygen," J. CHEM. PHYS., Vol. 90, 1986, pp. 466-471.

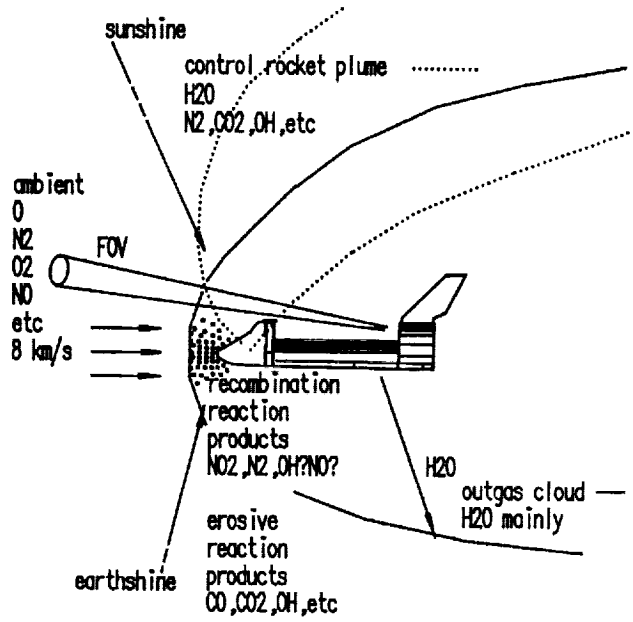

Figure 1. Sources of Contaminant Optical Radiations

Table I. Gaseous Optical Foregrounds from Spacecraft

LUMINESCENCE PROCESS	COMMENT
Gas-phase reactions between high kinetic energy desorbate/exhaust and atmosphere	Many reaction processes, with little quantitative guidance from experiment Large, separate topic
Surface-catalyzed recombination of atmospheric species	Multiple observations from space vehicles
Erosive/extractive reactions of incident species with exposed surface materials	Some laboratory data are now becoming available
Sunlight and earthshine pumping of gas cloud	Some evidence

Table II. Available Relative Kinetic Energy in Collisions with Exhaust Species.

Calculated for O :

Species	μ, amu	E_{max}, eV	E_{min}, eV
H_2O	8.47	5.74	0.45
N_2	10.2	6.91	0.55
H_2	1.78	1.20	0.092
CO	10.2	6.91	0.55
CO_2	11.7	7.92	0.62
H	0.941	0.64	0.050
MMH-NO_3	14.0	9.48	0.74
O_2	10.7	7.25	0.57
OH	8.27	5.60	0.44
O	8.00	5.42	0.43
NO	10.4	7.04	0.55
N_2H_2	10.4	7.04	0.55
NO_2	11.9	8.06	0.63
MMH	11.9	8.06	0.63
CH_2	7.47	5.07	0.28
CN_2H	11.5	7.79	0.61

Calculated for N_2 :

Species	μ, amu	E_{max}, eV	E_{min}, eV
H_2O	11.0	7.45	0.59
N_2	14.0	9.48	0.74
H_2	1.87	1.27	0.099
CO	14.0	9.48	0.74
CO_2	17.1	11.6	0.91
H	0.966	0.66	0.052
MMH-NO_3	22.3	15.2	1.19
O_2	14.9	10.1	0.79
OH	7.68	5.20	0.41
O	7.47	5.06	0.40
NO	14.5	9.82	0.77
N_2H_2	14.5	9.82	0.77
NO_2	17.4	11.8	0.93
MMH	17.4	11.8	0.93
CH_2	9.33	6.33	0.35
CN_2H	16.6	11.3	0.89

E_{max} / E_{min} : 3¼ km/s added/subtracted to 8 km/s orbital velocity

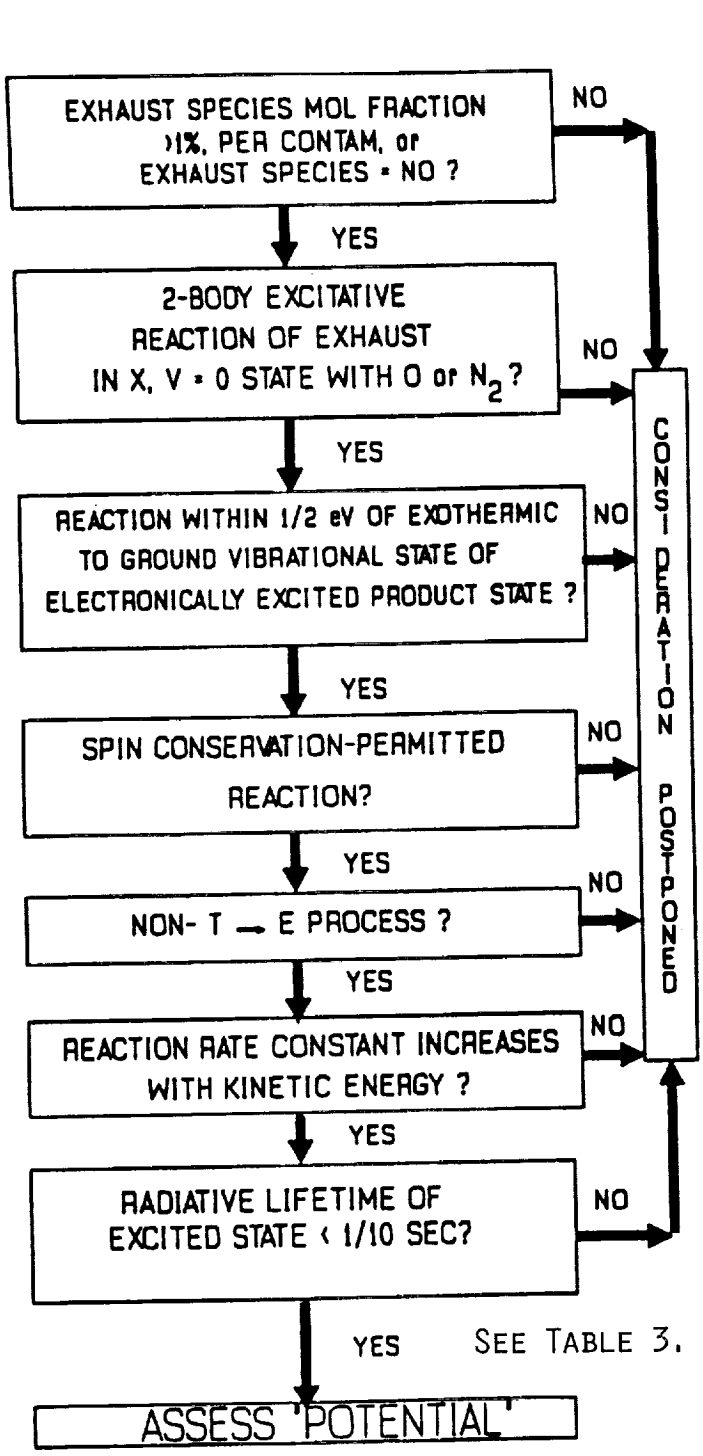

Comment/Caveat

Principally model prediction./ Unburned fuel, ions, droplets could be present.

Highest concentration ambient target species./ Reactions with O_2, ions, $N_2(v)$, $O\,^1D$ and $N\,^2D$ could play a part. Internal excitations of 3000K exhaust gas could contribute.

Rovibrational bands (principally IR) not considered./ Tail of velocity distribution could contribute.

Cross sections for reactions violating spin conservation are lower.

Cross sections for T → E processes are lower.

$O + NO \rightarrow NO_2^*$, for example, is exothermic with a rate constant that decreases with increasing relative kinetic energy.

Otherwise glow brightness reduced by delay of emission./ Energy transfer collisions could contribute.

Figure 2. Potential Foregrounds from Electronically Excitative Reactions from Exhaust Species

Table III. Exhaust gas reactions meeting the tests illustrated in Figure 2.

Reactants	Products	E_{th}, eV	E_{max}, eV	$\sigma(E_{max})$, Å^2†	Emission System †††
$H_2O(X) + O(^3P)$	$OH(A)^* + OH(X)$	4.83	5.74	0.19	~2400-3500Å
$CO_2(X) + O(^3P)$	$O_2(A)^* + CO(X)$	6.67	7.92	0.10	Herzberg I, ~2400-4900Å
	$O_2(B)^* + CO(X)$	8.45			Schumann-Runge, <1900Å
$NO(X) + O(^3P)$	$O_2(A)^* + N(^4S)$	6.07	7.04	0.06	Herzberg I, ~2400-4900Å
	$O_2(A)^* + N(^4S)$	7.85			Schumann-Runge, <1900Å
$CO(X) + N_2(X)$	$CN(A)^* + NO(X)$	≥7.70††	9.48	-----	Red, ~4400-15000Å
$CO_2(X) + N_2(X)$	$NO_2(A)^* + CN(X)$	≥10.75††	11.6	-----	Yellow-green-IR continuum
	$CN(A)^* + NO_2(X)$	≥10.04††		-----	~4400-15000Å

† Estimated as described in the text.
†† These figures are the endothermicities E_0 of the reactions. No information on the barrier threshold is available.
††† To ground state (X) of the excited molecule.

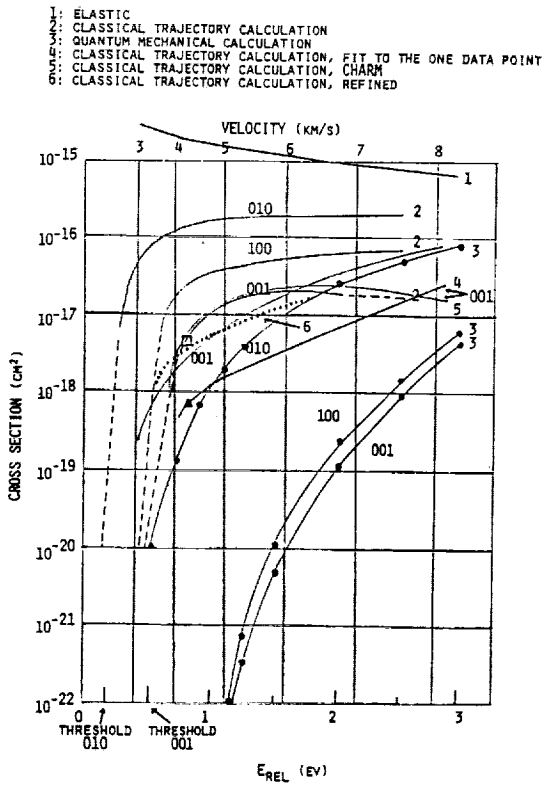

Figure 3. T→V in $O^3P + H_2O(X)$ collisions

Table IV. Principal Spacecraft Surface-Catalyzed Recombination Glows

Band System	$\Delta\lambda$	Spatial Extent*	Radiance**	Comments	Ref
N_2 Lyman-Birge Hopfield (a→X)†	1200-2100Å	6 cm	2 kR	Strong dependence on altitude unexplained	6
NO Beta (B→X)††	2400-3800Å	1¼ mm	1 kR	Excited at exposed sensor surfaces; A→X, C→X not observed	3
O_2 Herzberg I (A→X)	2500-4900Å	80 m	2 kR	Other recombinant O_2 states produce weak emission radiances	1
NO_2 pseudo-continuum ($^2B_1, ^2B_2 \rightarrow ^2A_1$)†	3900Å-2¼ μm	5-10 cm	10 kR	"Shuttle glow" from NO + O	5
N_2 Wu-Benesch (W→B), First Positive B→A††	1-3 μm & 5000-10000Å	4-40 cm (&¼ cm)	1 kR each	First Positive cascade follows W→B; A→X weak; other recombinant N_2 features weak also	1
NO $\Delta v = 2$	2.7-3 μm	100 m	$\frac{1}{4}\times10^{-13}$ w/cm^{2}ster	Vibrational cascade follows B→X, $v>0$	3
NO $\Delta v = 1$	5.3-6 μm	100 m	2×10^{-13} w/cm^{2}ster	Same as $\Delta v = 2$	3
NO_2 $\nu_1 + \nu_3$	3.4-3.8 μm	2¼ m	3×10^{-11} w/cm^{2}ster	Vibrational cascade follows X, ν_1,ν_2,ν_3	3
NO_2 ν_3	6.0-6.6 μm	2 m	4×10^{-10} w/cm^{2}ster	Strongest cascade component of NO_2	3

* (mean effusive desoption velocity)*(radiative lifetime of upper excited state).
** Nominal planning estimate, perpendicular projection, complete band system at 225 km altitude.
† Identified from spacecraft. †† Possible identification.

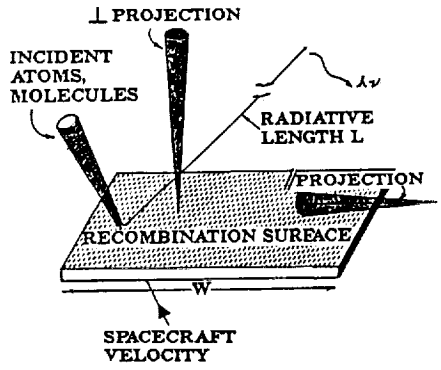

a) View Geometry

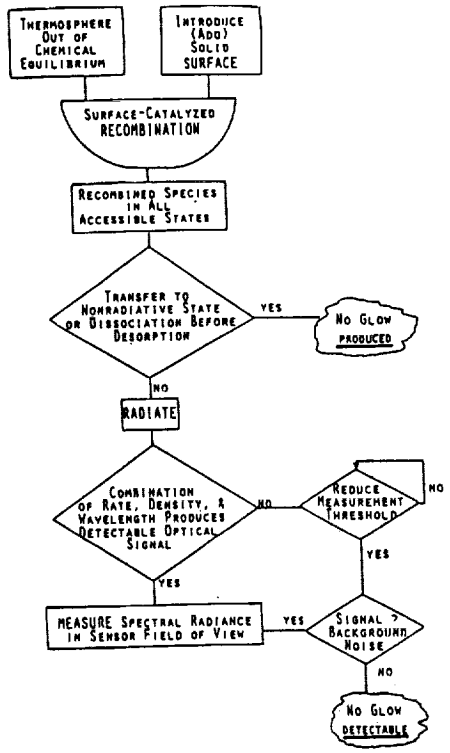

b) Conditions for production and detection of spacecraft off-surface glows

Figure 4. Conditions for Spacecraft-Induced Glows

Table V. UV Recombination radiations at low earth orbital altitudes

Recombinant Species	Upper Electronic States Accessible,* lifetime	Ultraviolet Band Systems Radiated	Radiative Pathlength**
$O^3P + O^3P \rightarrow O_2^*$	$\underline{A}\,^3\Pi_u^+$, 0.18 sec $\underline{A}'$(or c)$\,^3\Delta_u$, ~20 sec c, a, b	Herzberg I (→X) Herzberg II (Visible and IR)	80 m 10 km 5 - 100's km
$N^4S + N^4S \rightarrow N_2^*$	$a\,^1\Pi_g$, 120 μsec $A\,^3\Sigma_g$ with v ≃ 20, ~1000 μsec $A\,^3\Sigma_g$ with v ≃ 5, 2 sec $B\,^3\Pi_g$ a',B',W ~0.04, 10^{-5} and 10^{-3}-10^{-2} sec	L-B-H (→X) (→B, IR; B→A(v≃5), Vis & IR) Vegard-Kaplan Visible, but produces A, low v Mostly IR	6 cm 1 km
$N^4S + O^3P \rightarrow NO^*$	$\underline{B}\,^2\Pi$, 3.2 μsec A, 0.2 μsec C, 0.025 μsec a, b, 0.16 and 6 sec	β (→X) γ (→X) δ (→X) (Visible and IR)	1½ mm 1/10 mm
$NO + O \rightarrow NO_2^*$	$^2\underline{B}_1$, $^2\underline{B}_2$, 25-250 μsec	Pseudocontinuum, no UV component	1-10 cm

* Those underlined have been detected in the laboratory.
** Assuming the desorbate molecules have equilbrated-effusive desorption velocites.

Table VI. Infrared (≥ 8000 Å) Surface Recombination Species

Excited Molecule	Source	Comments
NO ($X^2\Pi$, v > 0)	Cascade from NO ($B^2\Pi$)	Present if β bands are excited, 2.7 and 5.3 μm
$NO_2(X^2A_1, \nu_1\nu_2\nu_3)$	Cascade from $^2B_{1,2}$ → X,v	Several band systems, strong; 3.6 and 6.2 μm, extending to 13 μm
NO_2 ($^2B_1$, $^2B_2$)	NO + O Recombination	Long-wavelength tail of pseudo-continuum extends to ~3 μm
$N_2(W^3\Delta_u)$	N + N Recombination	Inferred from laboratory results; Wu-Benesch (W→B) bands
$N_2(B^3\Pi_g)$	Cascade from W (or A) state	Seen in the laboratory; First Positive bands (B→A) extend into the near-IR
$O_2(a^1\Delta_g)$	O + O	IR Atmospheric bands (a→X) 1 hour radiative lifetime results in extremely low brightness
$O_2(b^1\Sigma_g^+)$	O + O	Near-IR Atmospheric bands (b→X) 12 sec radiative lifetime results in low brightness
$NO(b^4\Sigma^-)$	N + O	Near-IR Ogawa (b→a) bands; 6 sec radiative lifetime
$O_3(\nu_3)$	O + O_2	Not identified in laboratory; improbable, but if excited 001-000 at 9.6 μm, + hot bands